Heliyon 9 (2023) e13187

Contents lists available at ScienceDirect

Heliyon

journal homepage: www.cell.com/heliyon

Research article

Evaluation of neotectonic activity using watershed geomorphic analysis: A case study in the west of Dokan Lake, Kurdistan Region, Iraq

Lanja H. Abdullah [a,*], Hekmat S. Al Daghastani [b], Azhar Kh. S. Bety [a]

[a] *Department of Geology, College of Science, University of Sulaimani, Sulaymaniyah, KRG, Iraq*
[b] *Remote Sensing Center, University of Mosul, Mosul, Iraq*

ARTICLE INFO

Keywords:
Khrmallan valley
Morphotectonic mapping
Neotectonics
Morphometric indices
Khalakan anticline
Dokan lake
Kurdistan region Iraq

ABSTRACT

The Iraqi Kurdistan Region's landscapes are the product of a complex merging of the effects of the collision between the Arabian and Eurasian plates and various geomorphic processes. A study of the Khrmallan drainage basin in the west of Dokan Lake, based on a morphotectonic study is a significant contribution to our understanding of the Neotectonic activity in the High Folded Zone. This study investigated an integrated method of detail morphotectonic mapping and geomorphic indices' analysis for determining the signal of Neotectonic activity, using the digital elevation model (DEM) and satellite images. The detailed morphotectonic map, along with extensive field data, revealed considerable variation in the relief and morphology of the study area, and eight morphotectonic zones were recognized. The presence of a high anomalous value in stream length gradient (SL) ranges from 19 to 769, increasing the channel sinuosity index (SI) reaching 1.5, and the tendency of basin shifting through the transverse topographic index (T) ranging from 0.02 to 0.5, conclude that the study area is tectonically active. The strong relationship between the growth of the Khalakan anticline and the activation of faulting is concurrent with the collision of the Arabian and Eurasian plates. A hypothesis of an antecedent can be applied to the Khrmallan valley.

1. Introduction

The Earth's landscape is the time-integrated product of tectonics and climate changes, the first product creates topography and maintains relief [1–4]. However, the second product facilitates the erosional processes that, gradually, erode highland areas over time [5,6]. The landscape represents an important archive of the rates and spatial distribution of these deformations. Quantitative and qualitative analysis of such landscapes and unrevealing deformation from the landscape is made feasible through tectonic geomorphology [7–9].

Fluvial systems are most sensitive in their behavior and evolution, they hold a detailed record of past deformation in their shapes and morphology [10]. Anomalous values of geomorphic indices, especially, those concerning tectonics, have, frequently, been used as proxies for Neotectonic activity, in a variety of tectonically active areas and environments [7,11–16]. The recent development in technology and advances in computer programming languages, Geographic Information Systems (GIS), and remote sensing techniques with the availability of topographic data from the (DEM) made tracking these activities easier and more effective [17–30].

* Corresponding author.
E-mail address: lanja.abdullah@univsul.edu.iq (L.H. Abdullah).

https://doi.org/10.1016/j.heliyon.2023.e13187
Received 12 September 2022; Received in revised form 14 January 2023; Accepted 19 January 2023
Available online 23 January 2023
2405-8440/

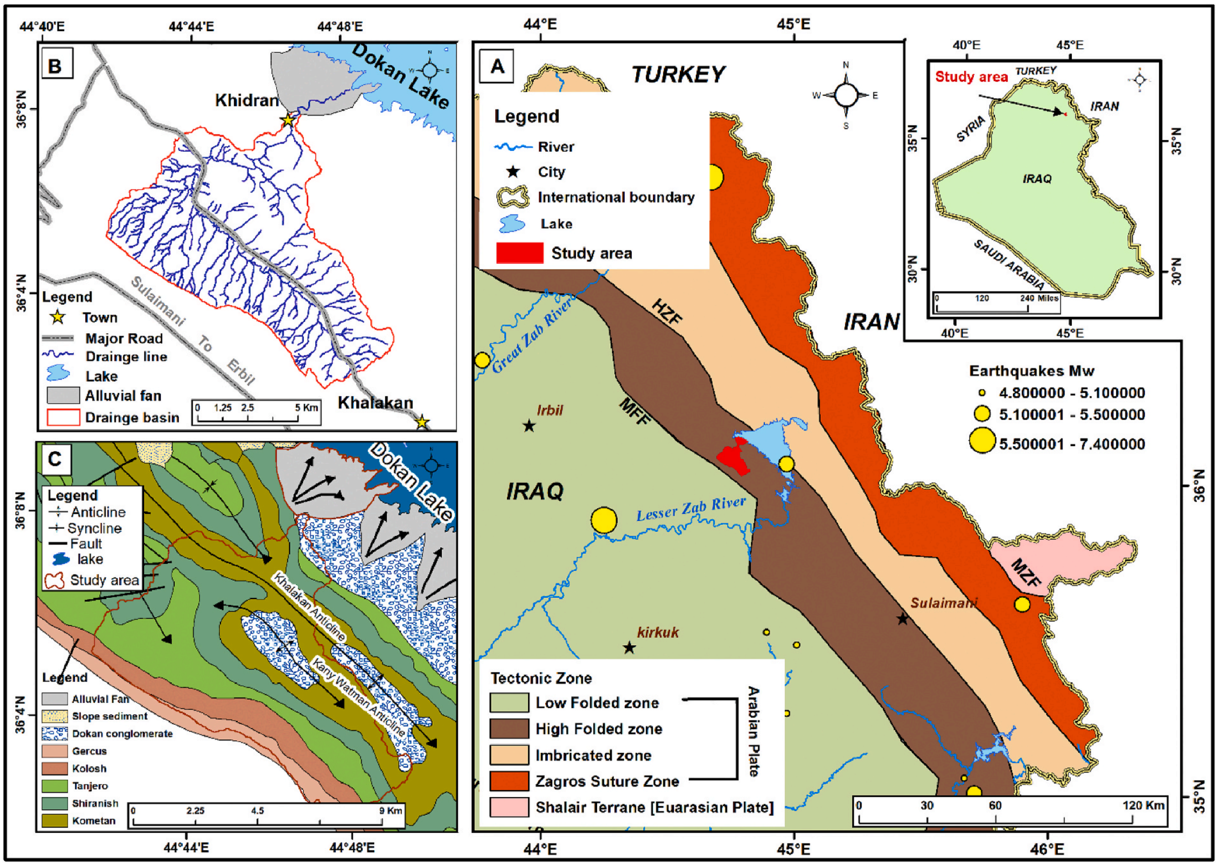

Fig. 1. The study area (A) is a tectonic map [42]. (B) A Drainage basin boundary with drainage lines. (C) A geological map [105].

Many previous studies highlighted the influences of tectonics in the development of anticlines, faults, effects on the vergency of the plunges, and their geometry related to paleo stresses, and stratigraphic sequences, however, none has focused specifically on how to detect tectonic activity through morphometric indices [31–43].

The current research is a case study of the Khalakan anticline, Khrmallan valley, and the associated alluvial fan, all located in the High Folded Zone (HFZ), which is affected by compressive strength, accordingly, influencing the growth of the folds in the Zagros Foreland Basin; due to the collision of the Arabian and Eurasian plates [44–47]. This research aims to detect the local tectonic activity and track the deformation marker resulting from faulting or folding through remotely sensed data by analyzing the morphometry of basins and their drainage networks as a tectonically induced landform [48,49]. Moreover, to determine if there is any uplifting and tilting, by producing a detailed morphotectonic map and analyzing morphometric indices of the main drainage basin, farther more this study can be used by the decision maker for any plan. Therefore, we conducted a comprehensive morphologic analysis of the Khrmallan drainage basin including these morphometric indices: stream length gradient (SL), channel sinuosity (SI), and transverse topographic index (T), besides constructing alluvial fan radial profile analysis, visual interpretation, and local field observations.

2. Geological and seismotectonic setting

The northeastern part of the Outer Platform of the Arabian Plate is within the Zagros Fold-Thrust Belt (ZFTB) [46]. This belt is considered active and is situated within the Arabia-Eurasia collision zone [50–52]. The oblique NE convergence of the Arabian and Eurasian plates during the Late Cretaceous is at a rate of 20–24 mm/yr [53,54]. The activity of the compression phase of these two plates is studied through various disciplines [55–58].

This ZFTB represents the most deformed part of Iraq, it has an NW – SE trend with an extension from the northwestern to southeastern parts of Iraq [47,59]. The ZFTB consists of four zones: Suture, Imbricate, High-Folded, and Low-Folded zones [46] (Fig. 1A). The study area is framed in the High Folded Zone (HFZ) in the Kurdistan Region of Iraq, west of Dokan Lake (Fig. 1 A, B). The HFZ was formed by the Zagros deformation during the Late Cenozoic [59] and uplifted in the Cretaceous, Paleocene, and Oligocene periods [55] and is still active [46,58,60,61]. Folds in the HFZ are characterized by NW-SE trending and SW-verging fault-related folds [62].

The anticlines in the HFZ are long and narrow, asymmetric, and separated by narrow and shallow synclines. The folds are probably controlled by thrust faults [63,64], and most of them are fault-propagated folds and some of them are fault-bend folds, with local overturning limbs [39]. Most earthquakes are caused due to the reactivation of preexisting faults within the Late Precambrian

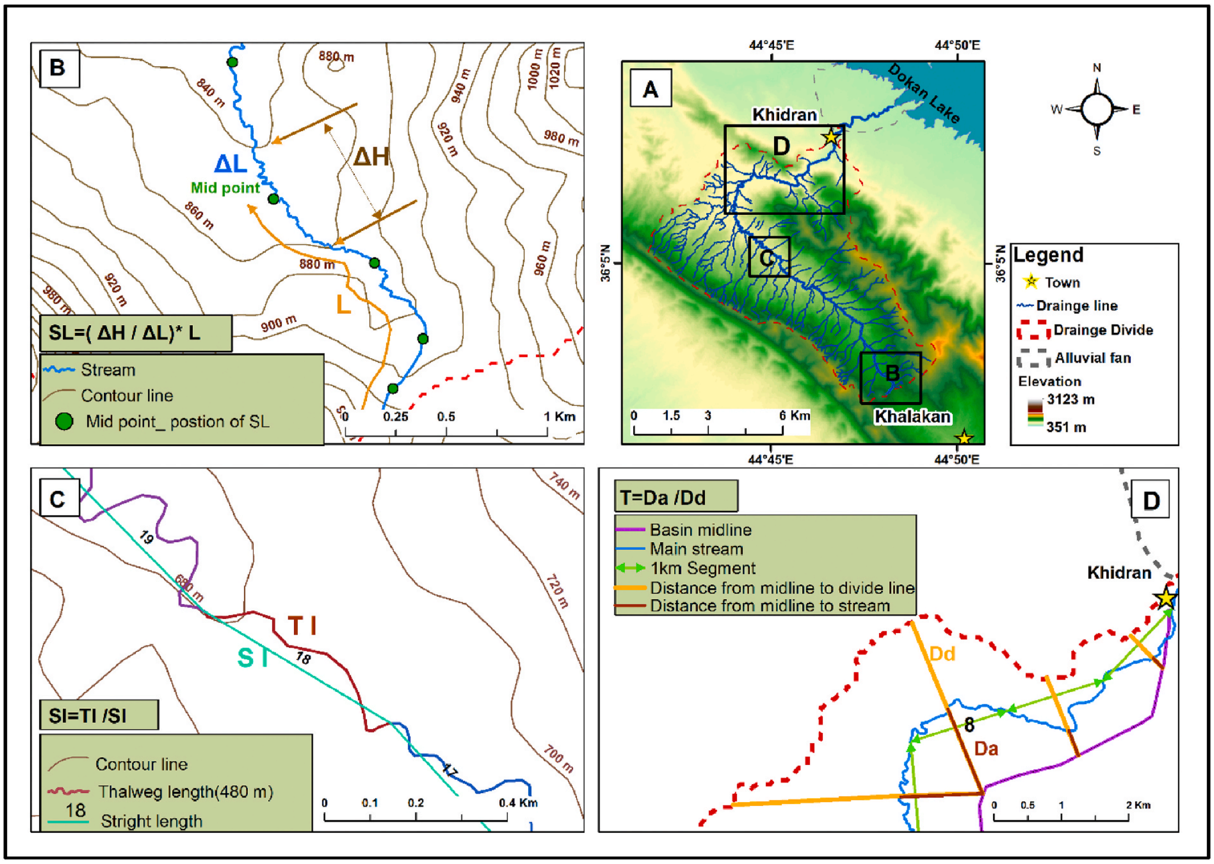

Fig. 2. (A) DEM shows the main tributary of the Khrmallan stream with three subsets, (B) finding stream length gradient (SL), (C) finding Channel sinuosity index (SI), and (D) finding transverse topographic index (T).

Basement [65–68]. The study area's seismicity was considered moderate to high [69]. Documentation about large-magnitude earthquakes indicates the activity of these faults [70–73].

The exposed rocks in the study area are of the Cretaceous and Neogene ages besides various types of Quaternary sediments. The exposed formations from the oldest to youngest are the Qamchuqa, Kometan, Shiranish, Tanjero, Kolosh, Gercus formations, and Dokan Conglomerate [31,38,105] or Khalakan formation [42] (Fig. 1C).

3. Materials and methods

DEM—Shuttle Radar Topography Mission (SRTM) at a resolution of 1 arc-second (~30 m), and different imageries from Quick Bird with 0.5 m resolution, Sentinel 2 imagery, and Rapid Eye with 5 m resolution have been used for visual interpretation and geomorphometric analysis, besides the usage of the geological, topographical maps at scales of 1:100,000, and earthquake data for 22 years ago from 2000 to 2022. Drainage basins and the associated network were generated with the aid of MATLAB base TecDEM software [27]. Metadata for the sub-basins, morphometric parameters, and final map preparation were all compiled in ArcGIS 10.5.1. Furthermore, a field check was carried out to confirm the observed and detected evidence of active tectonics in the studied area. Three geomorphic indices; SL, T, and SI have been analyzed; a detailed methodology is illustrated in (Fig. 2A-D). For calculating SL values, the main streamline was overlaid with 20 m contour lines converted from the DEM, and ΔH was assigned with an equal contour interval = 20 m following [1,7,14,74] (Fig. 2B). Furthermore, a GIS Toolbox (SLiX), which was suggested by Piacentini et al. [29] was used for computing SL values, automatically, but we have not considered these values in our analysis because this method follows the regular spacing of stream segments for computing ΔL and this will lead to hiding the anomalous values.

The T index was calculated for each midpoint of the 1 km segment length of the main streamline, which is at least twice the width of the meander belt [75], and the midline of the basin was determined by the river bathymetry tool proposed by Bailey et al. [76]. The T index values have magnitude and direction, so these data were plotted on polar diagrams to reveal the migration trends (Fig. 2 D). The SI index was calculated by fixing the measured channel distance (thalweg length), whereas the valley distance (straight line) varies depending on the sinuosity of the stream [77–79](Fig. 2 C).

The International Institute for Areal Survey and Earth Sciences (ITC) classification system [80] was used for detailed morphotectonic mapping on a scale of 1:60,000. The first step started from a regional scale based on a conceptual and geomorphological

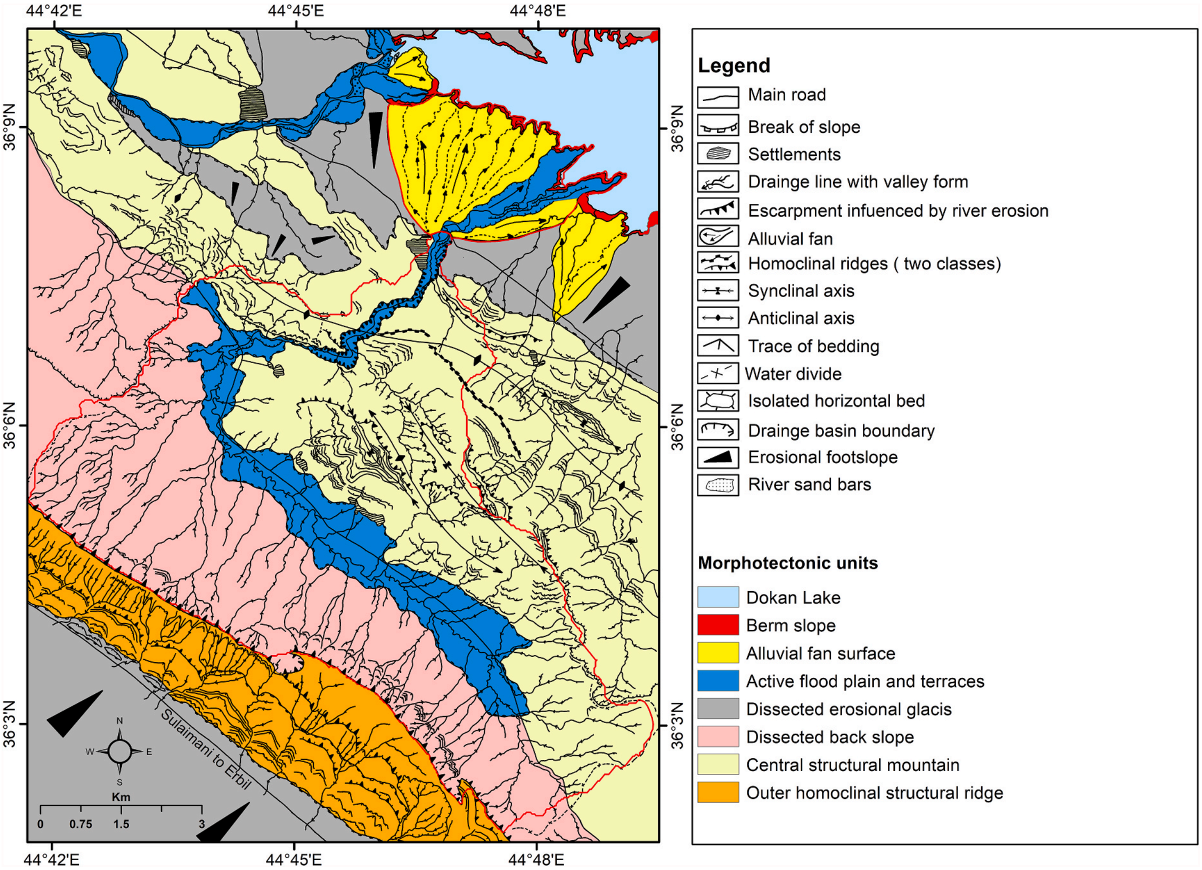

Fig. 3. Detailed complied morphotectonic map of the study area, the red thin line showing the limits of the basin. (For interpretation of the references to colour in this figure legend, the reader is referred to the Web version of this article.)

approach to have the main units. The second step was manually drawing and classifying the study area on (A0) trace paper covering the satellite images of the study area. The third step was field verification and editing of the map, and the last step was digitizing, coloring, and extracting the final layout in an ArcGIS environment (Fig. 3). Although the geomorphic indices can be used for mapping large areas, our applied method will be applicable for small drainage basins because calculating the SL index in that precise way (according to contour spacing), will be difficult for a large number of streams, and drawing such a detail morphotectonic mapping based on visual interpretation will need more time and the scale limitation will not allow to draw and differentiate these units boundaries.

4. Morphotectonic zones mapping

High-resolution satellite imagery and the DEM were visually interpreted to delineate the main morphotectonic zones, which mainly reflect the articulated, tectonically controlled geomorphological evolution of the study area. Based on the ITC terrain classification [80], the study area was divided into eight major units depending on the relief, lithology, process, and genesis of the terrain.

The main morphotectonic units are described as they appear in the map legend (Fig. 3):

1. Dokan Lake: This zone represents the area covered by the Dokan dam reservoir. 2. Berm slope: This zone is developed in response to the change and fluctuation of water levels and wave actions. 3. Alluvial fan: This zone is representing the recent alluvial sediments deposited by the Khrmallan stream after crossing the Khalakan anticline, the shape of the alluvial fan reflects the neotectonic history in the area. 4. Active flood plain and terraces: This area is characterized by the lowest aggradation surface found along active stream beds. The river terrace levels are traced along both streamsides, but not chronologically separated, due to the scale limitation of the map. 5. Dissected erosional glacis: This zone represents the residual ridges and is characterized by the bedding trace of alternating sequences of resistant and non-resistant rocks, covered by unconsolidated Quaternary sediments. 6. Dissected back slopes: This zone shows the denudational cliffs of the back slopes belonging to the outer homoclinal ridges. 7. Central structural mountain: This zone represents the core of the anticline as a high topographic unit occupied by the highly resistant rock of the Qamchuqa Formation and Dokan conglomerate. 8. Outer homoclinal structural ridge: This zone represents the homoclinal structure on the northwestern side of the basin boundary. This ridge is recognized due to the deferential weathering of the alternating lithology and the effect of subsurface thrust faulting of the Khalakan anticline.

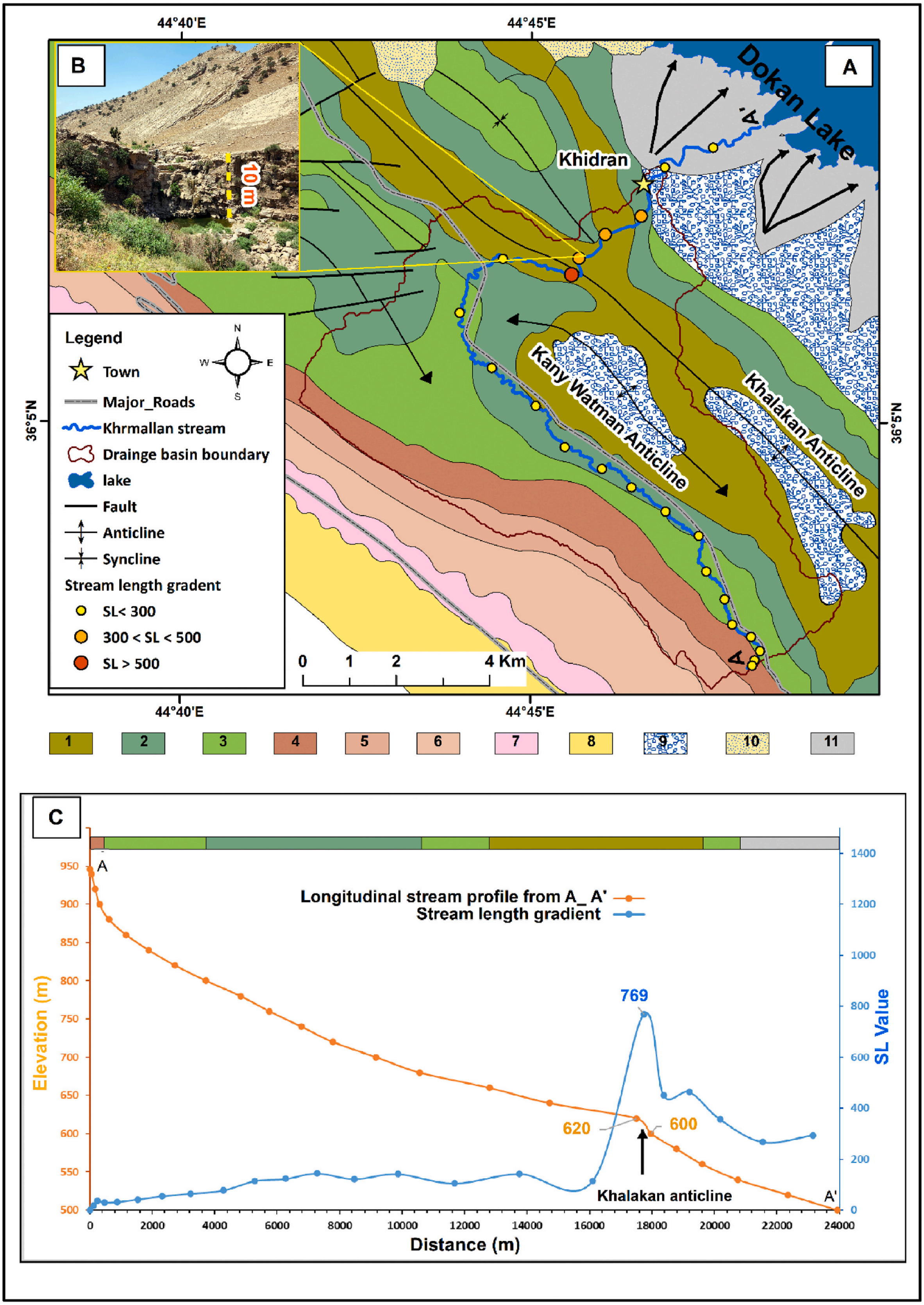

(caption on next page)

Fig. 4. (A) Geological map showing; SL index values for the Khrmallan stream and their relationships to bedrock lithology (Formations:1. Kometan 2. Shiranish, 3. Tanjero, 4. Kolosh, 5. Gercus, 6. Pila Spi,7. Fatha, 8. Injana, 9. Dokan Conglomerate,10. Slope sediments, 11. Alluvial fan sediments) [105]. (B) Badwan Waterfall. (C) A graphic plot between the stream long profile and SL values shows a significant change along with these high anomalous SL values.

5. Results

5.1. Stream length-gradient index (SL)

A total of 22 SL values along the Khrmallan stream were computed (Fig. 2B), ranging from 19 to 769. This index is classified into three classes [81]: High: SL > 500, Moderate :300 ≥ SL < 500, and Low: SL < 300 (Fig. 4 A, C). Moderate and low values along the streamline are related to the occurrence of a geomorphic disequilibrium, while the highest anomalous values (769) (as shown above)

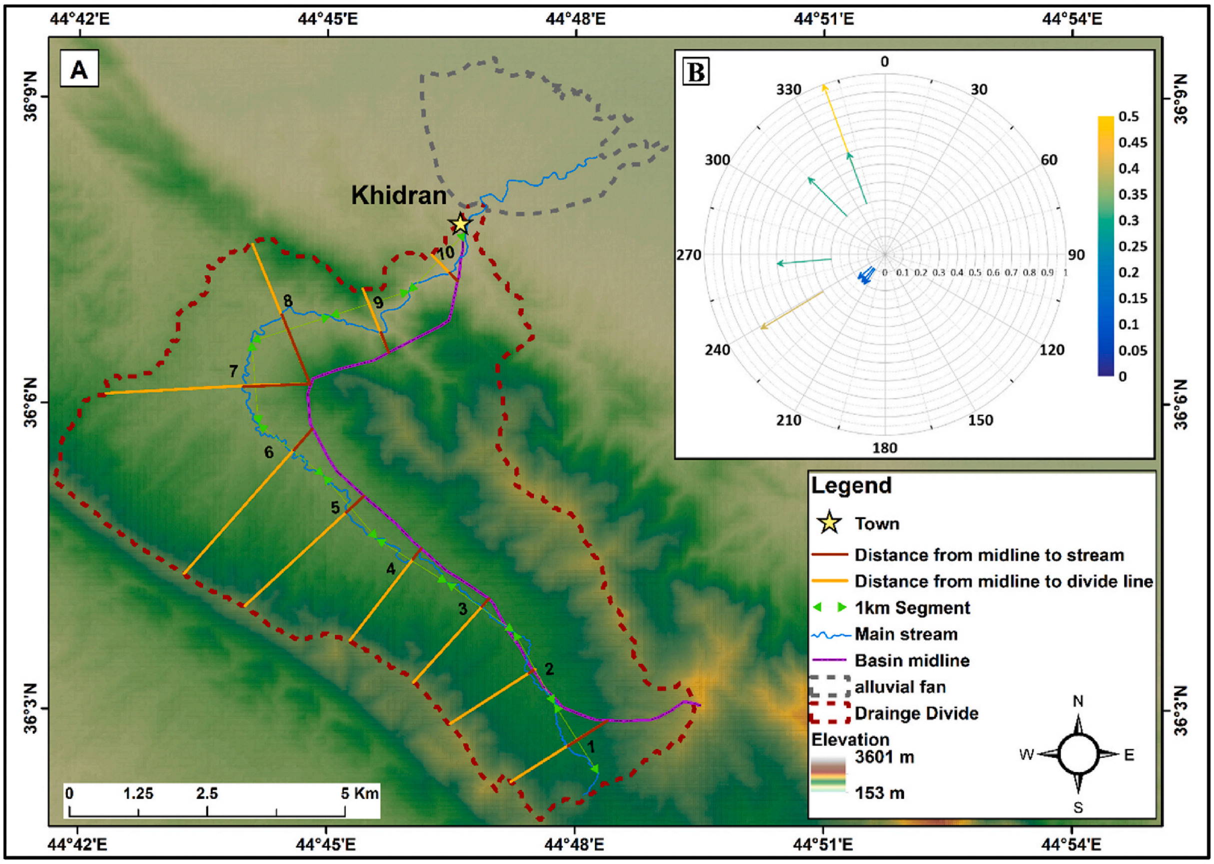

Fig. 5. (A) DEM shows the calculated T index along the segmented river. (B) Polar plot showing T index along the mainstream channel and showing the azimuth of stream deflection from basin midline.

Table 1
The magnitude and azimuth direction of each segment of the mainstream.

Segment Number	Da	Dd	T	Azimuth direction
1	0.9	2.1	0.4	239°
2	0.1	1.8	0	235°
3	0.2	2.0	0.1	220°
4	0.3	2.1	0.1	215°
5	0.4	2.9	0.1	228°
6	0.5	3.5	0.1	220°
7	1.2	3.7	0.3	265°
8	1.4	2.7	0.5	340°
9	0.4	1.3	0.3	340°
10	0.2	0.7	0.3	315°

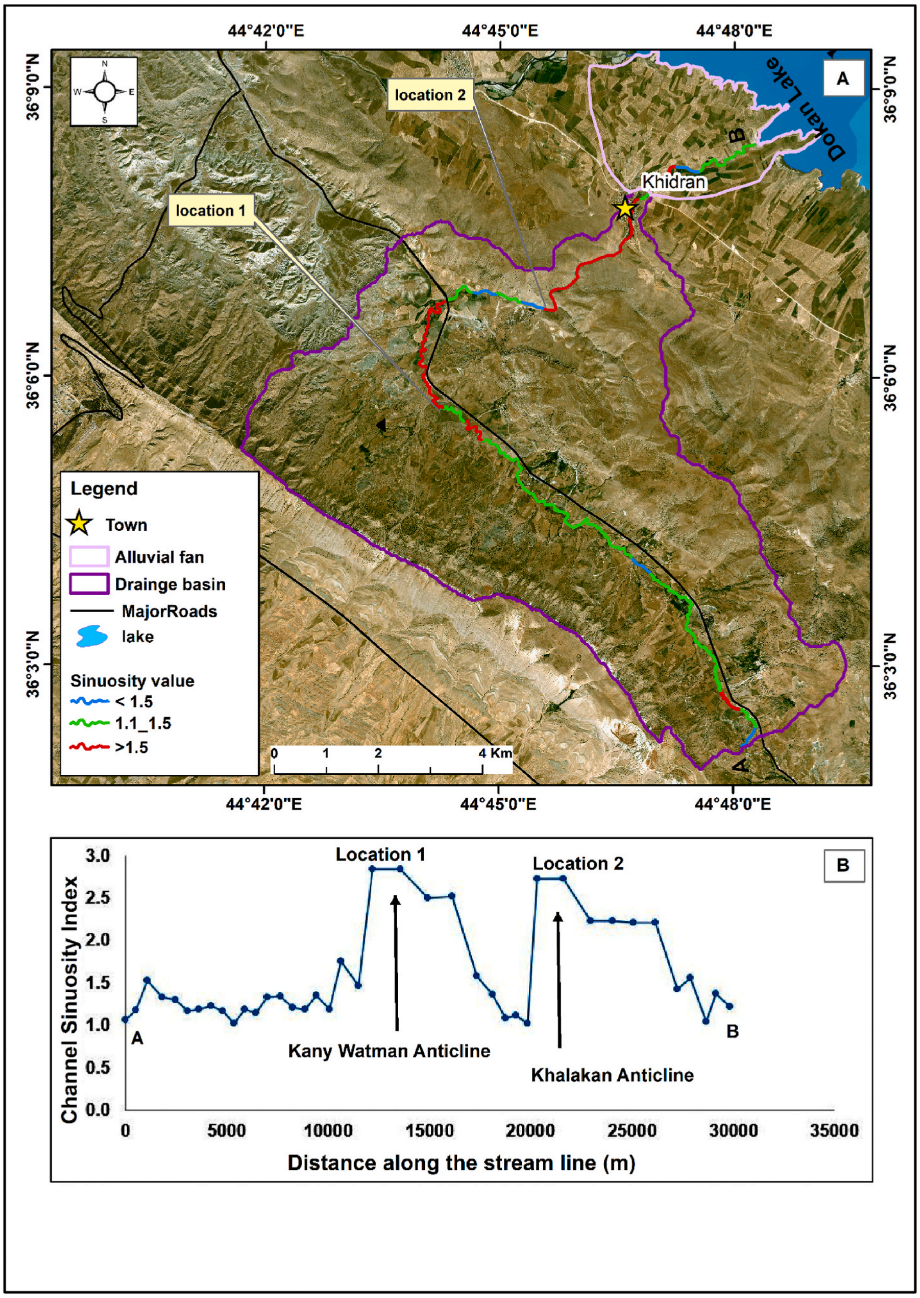

Fig. 6. (A) Satellite image showing (SI) values along Khrmallan stream. Note the changes in river sinuosity at the indicated locations (1 and 2). (B) Graphical plot of sinuosity index values and stream distance from A to B.

are related to tectonic activity, and can be found in the NW of Khidran town. The constructed longitudinal stream profile in (Fig. 4C) also shows irregularities in the form, which means that the profile is no longer in a steady state.

5.2. *Transverse topographic index (T)*

To reveal possible patterns of ground tilting in the studied area, we examined the lateral stream migrations from the basin midline; quantitatively. According to Cox [75] (Fig. 2D), the computed values of the T-index range from 0.02 (perfect symmetry) to 0.5 (asymmetry) (Fig. 5 and Table 1). The high T-index value (0.5) shows shifting in a perpendicular direction to the drainage basin axis around the Kany Watman anticline NW plunge area (Fig. 5A, B). The shifting tendency of the vector plot on the polar graph from SW to NE shows the level of tectonic asymmetry, assuming that the dip of the bedrock has negligible influence on the migration of stream

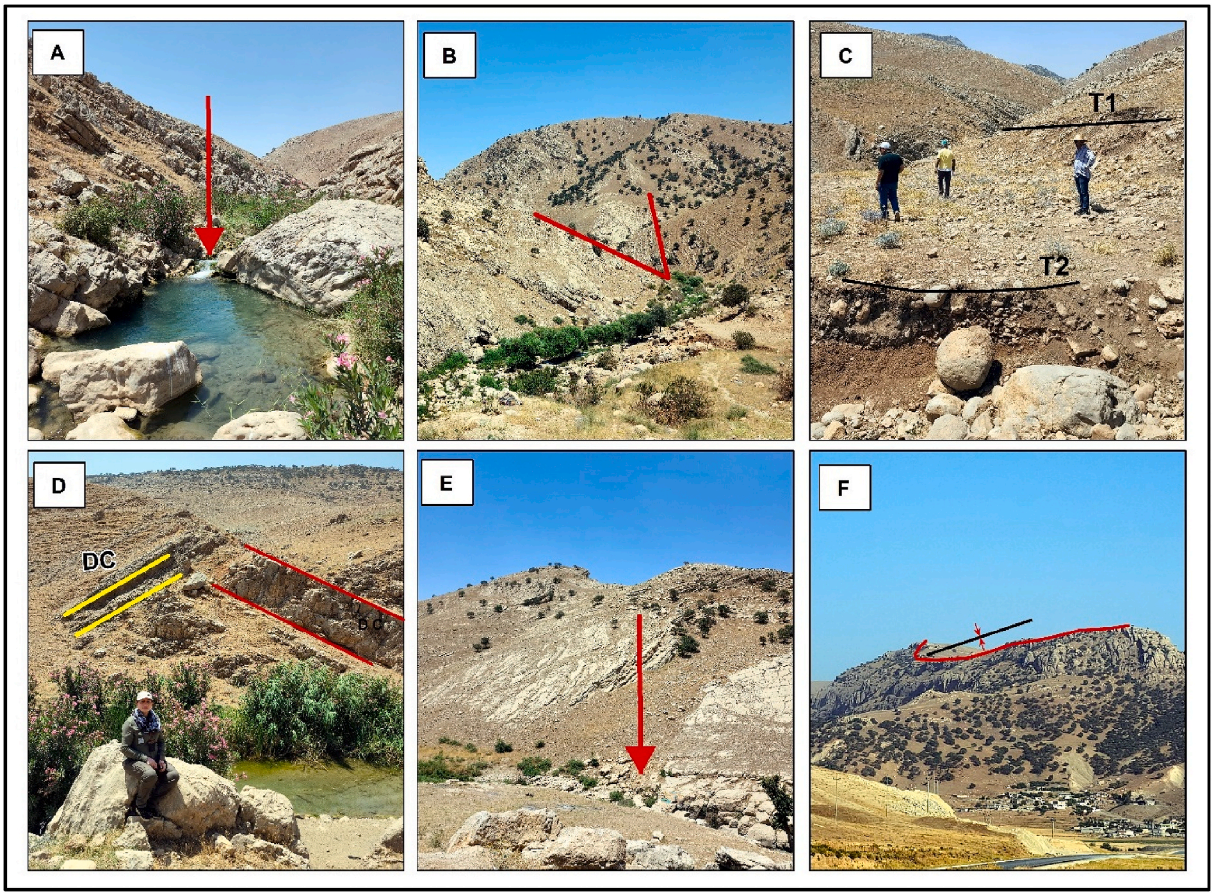

Fig. 7. Field evidence of the tectonic activity in the studied area. (A) Water gap crossing Khalakan anticline, (B) a Narrow V-shaped cross-section in the knickpoint place, (C) Two-stage of terraces downstream of the gorge, (D) Dokan conglomerate (DC) angularly overlying Qamchuqa formation, (E) migrated nick point in the upstream side of the waterfall, (F) Hanging syncline over Kany Watman anticline.

channels according to the field observation.

5.3. Channel sinuosity index (SI)

According to Schumm [104] (Fig. 2C), the calculated SI values were divided into three classes (SI:1–1.05 is Straight, SI:1.06–1.30 is Sinuous, and SI:1.31–3 is Meandering). Fig. 6 A, B shows that the sinuosity is increasing as the stream adjusts its pattern to maintain the constant gradient over the slope of the changing valley floor. This was recognized when the stream reaches the NW plunge of the growing anticline and crosses the Khalakan anticline.

6. Neotectonics evidence in the Khrmallan valley

Despite the clear geomorphic analysis response to the tectonic signal, some observed evidence along the Khrmallan valley appears to represent a system that has evolved and reflects a very complicated system, indicating Neotectonic activity in the study area.

The crossing of the Khrmallan stream over the Khalakan anticline, forming a typical water gap and acting as an antecedent stream, is a good indication of Neotectonic activity [82,83] (Fig. 7A). The presence of a deep incised V-shape valley without any fluvial deposits in the gorge, while the availability of fluvial terraces in the bank of the stream before and after passing the gorge with wide and U-shaped valley is indicating that the uplifting rate is greater than the depositional rate (Fig. 7B, C). Another evidence can be represented by the overlying of the Dokan Conglomerate to the Kometan Formation in angular unconformity along the overturned NE flak of the Khalakan anticline and showing a recent tilting (Fig. 7D). The availability of migrated Knickpoints on the upstream side of the major knickpoint shows the rate of geomorphic response to tectonic and climatic perturbation (Fig. 7E). The growing set of hanging synclines and anticlines in the horizontally laying Dokan conglomerate over the main anticline can be represented as evidence of Neotectonic activity in the area (Fig. 7F).

Furthermore, the associated alluvial fan of the Khrmallan stream was analyzed, and four radial profiles and two cross profiles have been constructed (Fig. 8 A-C). The radial profiles have different slopes degree and the transverse profiles show a convex curve with

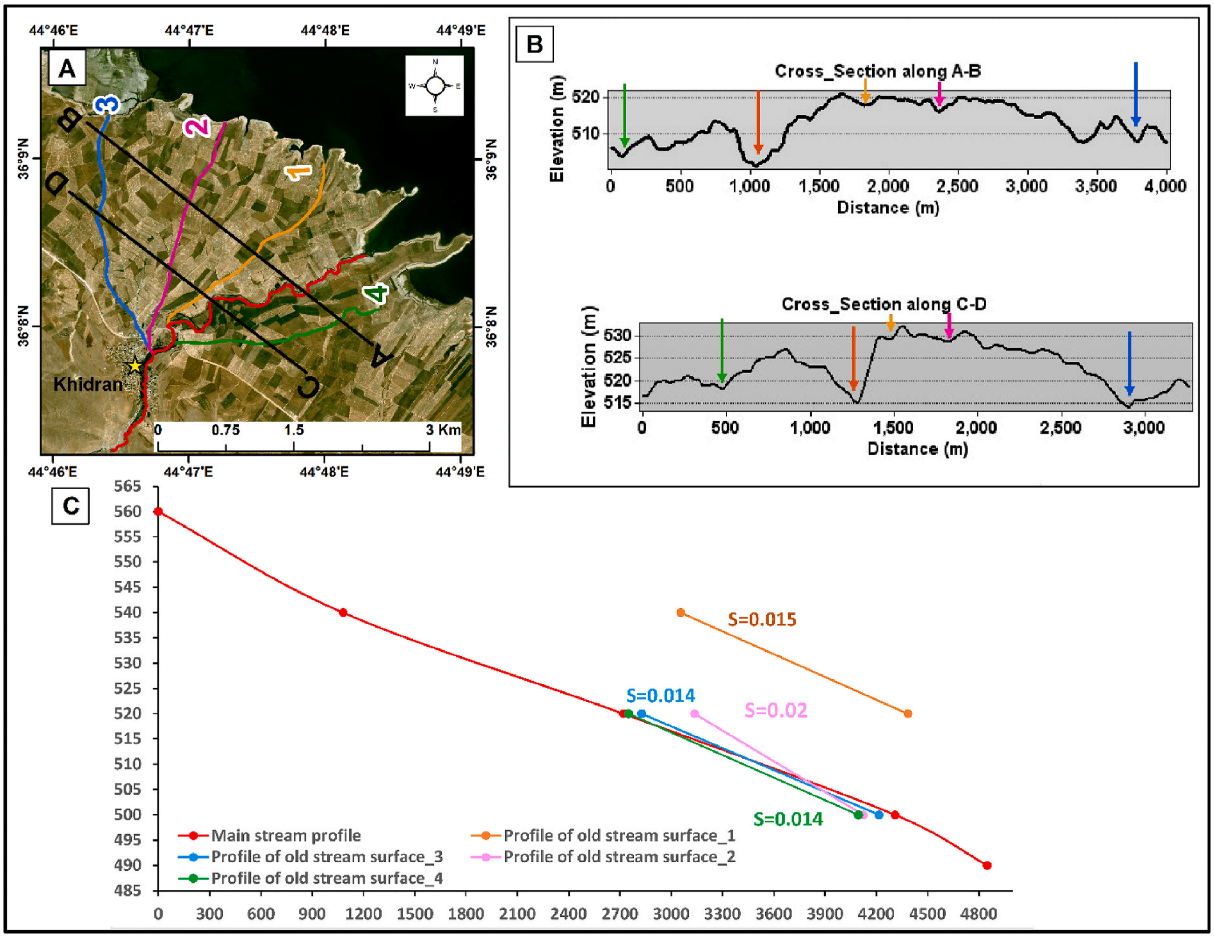

Fig. 8. (A) Satellite image illustrating the associated alluvial fan of Khrmallan stream, the coloured lines with number show old incised stream channels. (B) Cross-section profile along A-B and C-D lines, the coloured arrows refer to the incision locations. (C) Altimetric and spatial arrangement of the alluvial fan's old incised stream profiles as compared with the mainstream profile, (s) denote the slope of the profiles.

steep breaks due to the existence of deep new and old incised stream channels (Fig. 8C). The profiles of the main incised stream channels; from the apex to the toe of the fan and the fan radial surface's profile were correlated and clearly showed the overall convergent geometry downstream, which is a good indication of Neotectonic activity in that area.

7. Discussion

A detailed geomorphological investigation through qualitative analysis of three geo-morphic indices and detailed morphotectonic mapping indicated that Neotectonic activity is prevailing in the Khrmallan drainage basin, and this activity plays a key role in the changing of geomorphometric properties of the drainage basin and surrounding area.

Determining tectonic activity through a geomorphological signal and using remotely sensed data represent one of the recent fo-cuses of the researchers, and correlating with other disciplines will improve the research quality.

The compiled morphotectonic map demonstrates a strong correlation between stratigraphic and tectonic activity and reflects a complex and dynamic adjustment of the Khrmallan drainage system induced by Neotectonic activity, because of the scale limitation we couldn't draw some landforms like landslides, erosional and depositional form.

The analysis of geomorphic indices of the Khrmallan drainage basin reflects the significance of the Neotectonic activity.

The SL index analysis along the Khrmallan stream shows an anomalous value (knick-point) on the elevation of (600–620) m above sea level and is recognized in the field as a (10 m) high "Badwan waterfall" near Khidran town (Fig. 4) which is related to the tectonic activity of Khalakan anticline.

Furthermore, the SL values were combined with a longitudinal stream profile (Fig. 4C), for showing the sensitivity of the drainage basin to tectonic deformation [84–88]. From the stream profile shape, we note the presence of a sharp Knick point adjacent to the Khalakan anticlinal axis. The analysis met our expectations through the SL index analysis and the narrow and deep valley in that area indicates that the high rate of incision is associated with the tectonic uplift of the khalakan anticline through activation of thrust faults

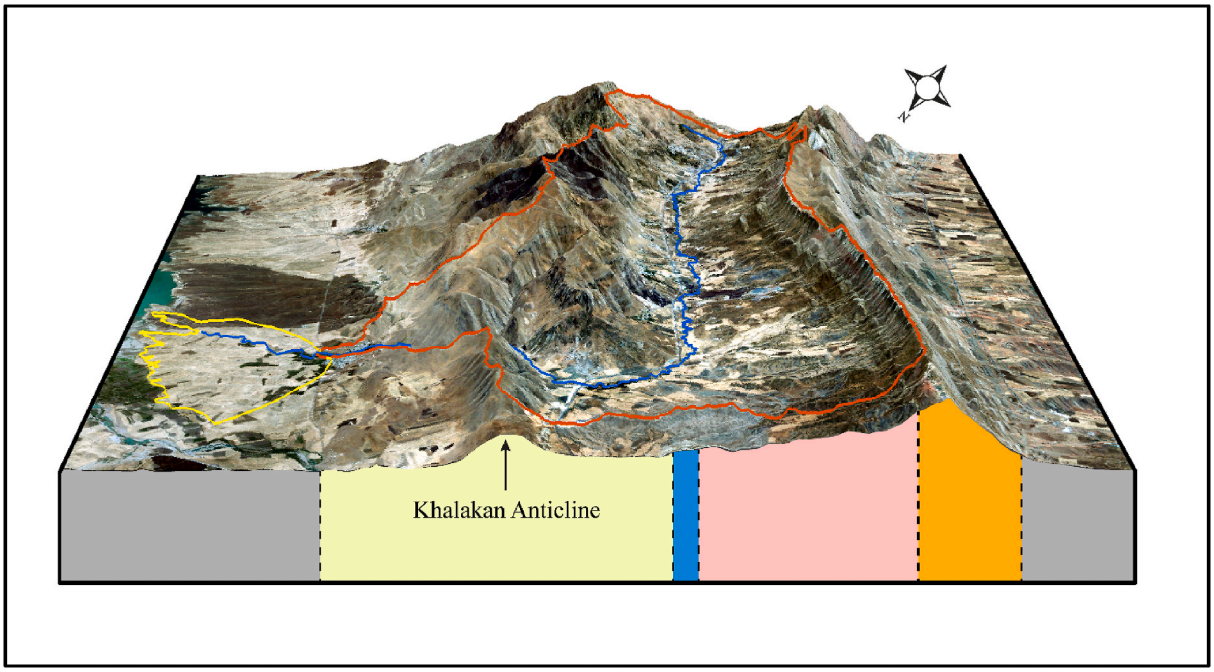

Fig. 9. A simple conceptual model showing the evolution of Khrmallan valley and growing of Khalakan anticline (for morphotectonic unit's colour refer to (Fig. 3). (For interpretation of the references to colour in this figure legend, the reader is referred to the Web version of this article.)

reported by Ref. [42].

To determine whether the anomalous SL values in the main profile are attributable to lithological control [89]or tectonic controls [7,8], the cross-validation was done by combining lithology, and SL values (Fig. 4A, C). The SL values show a significant variation within one lithological unit. Therefore, we suggest that these knickpoints are not related to the lithological change.

The possibility of the ground tilting of the drainage basin and lateral shifting tendency were detected through T index analysis, the Khrmallan stream course shows a 90° bending from the flowing NW ward parallel to the Khalakan anticlinal axis to the NE ward. The shifting tendency of a stream in the active tectonic region is confirmed by [90–93], This can be probably caused by the combination of a set of growing folds and reactivation of faults [37,39,43,94,95].

The channel morphology and sinuosity were analyzed through the SI index, which shows a change in valley floor slope as the first response to back-tilting and most probably due to the tectonic activity of the Khalakan anticline. The effect of fold and domal uplifting on increasing the sinuosity values of the channel pattern adjustment to maintain the equilibrium has been also reported by other works [1,88,96–102].

Through all these analyses, it is clear that the Khalakan anticline is still active and growing and coincides with the hypothesis of the antecedent stream and fold growing [38,40]. The recorded seismological activities in the area and surrounding contribute to a clearer understanding of these tectonic activities. This may be because of the activation of blind thrust faults as previously confirmed by Berberian [50] and De Vera et al. [103]. The study provides new insight into the relationship between remotely sensed data and detecting Neotectonic activity in any area and the reliability of this work will be impacted by using high-resolution data and field checks.

8. Conclusions

The sum and combination of the obtained results allowed us to conclude that the integration of morphotectonic analysis with geoinformatics and remote sensing technology can detect the ongoing surface and subsurface Neotectonic activities over the Khrmallan drainage basin.

Detailed morphotectonic analysis and extensive Neotectonic activity in the area were comprehensively studied for the first time. Meanwhile, the outcome of this investigation can help the decision maker about any future planning like the classification of landscape based on tectonic activity, and may also serve as a structural framework facilitating local planning of infrastructures. We determine the Neotectonic activity of the Khrmallan drainage basin and the activity of these movements is still ongoing and leading to the growth of Khalakan anticline, and acting as an antecedent stream (Fig. 9).

In summary, we analyzed the morphotectonic growth of the Khrmallan drainage basin and the existence of Neotectonic activity, are matched our expectation that the main ZFTB as a consequence of oblique convergence between the Arabian and Eurasian plates, has played an important role in shaping the study area during a multi-stage de-formational evolution. Future studies on the Quaternary chronology of the river deposits might confirm and enrich our conclusions.

Author contribution statement

L. H. Abdullalh: Conceived and designed the experiments, Performed the experiments, Analyzed and interpreted the data, Contributed reagents, materials, analysis tools, or data and wrote the paper. H.S. Al-Daghstani: Conceived and designed the experiments, Analyzed and interpreted the data, and Contributed reagents, materials, analysis tools, or data. A. Kh.S. Bety: Analyzed and interpreted the data and Contributed reagents, materials, analysis tools, or data

Funding statement

This research did not receive any specific grant from funding agencies.

Data availability statement

All the data used during this study appear in the submitted article, other related data will be available from the corresponding author upon reasonable request.

Declaration of interest's statement

The authors declare no competing interests.

Additional information

There is no data saved in a special repository.

Acknowledgements

This is a part of the doctoral thesis of the graduate program in the Geology Department of the University of Sulaimani. We are grateful to Dr. Kamal H. Karim and Dr. Ghafor A. Hamasur for their help during the fieldwork. We also thank Dr. Arsalan A. Othman, Mr.Jabbar M. Qaradaghi, and Mr. Sardar S. Fatah for their assistance. We would like to thank the USGS and NASA for the free data used in this study. We would like to express our sincere thanks to the reviewers for their valuable comments.

References

[1] C. Wobus, K.X. Whipple, E. Kirby, N. Snyder, J. Johnson, K. Spyropolou, B. Crosby, D. Sheehan, Tectonics from topography: Procedures, promise, and pitfalls, Spec. Pap. - Geol. Soc. Am. 398 (2006) 55–74.
[2] K.X. Whipple, Bedrock rivers and the geomorphology of active orogens, Annu. Rev. Earth Planet Sci. 32 (2004) 151–185.
[3] A.C. Whittaker, M. Attal, P.A. Cowie, G.E. Tucker, G. Roberts, Decoding temporal and spatial patterns of fault uplift using transient river long profiles, Geomorphology 100 (2008) 506–526.
[4] R.A. Hartley, G.G. Roberts, N. White, C. Richardson, Transient convective uplift of an ancient buried landscape, Nat. Geosci. 4 (2011) 562–565.
[5] P.A. Allen, From landscapes into geological history, Nature 451 (2008) 274–276.
[6] J.J. Armitage, R.A. Duller, A.C. Whittaker, P.A. Allen, Transformation of tectonic and climatic signals from source to sedimentary archive, Nat. Geosci. 4 (2011) 231–235.
[7] E.A. Keller, N. Pinter, Active Tectonics Earthquakes, Uplift, and Landscape, 2nd ed., Prentice Hall, Upper Saddle River, 2002.
[8] E. Kirby, K.X. Whipple, Expression of active tectonics in erosional landscapes, J. Struct. Geol. 44 (2012) 54–75.
[9] D.W. Burbank, R.S. Anderson. Tectonic Geomorphology, 2nd ed.,A, John Wiley & Sons, Ltd, 2001.
[10] K.X. Whipple, E. Kirby, S.H. Brocklehurst, Geomorphic limits to climate-induced increases in topographic relief, Nature 401 (1999) 39–43.
[11] W.B. Bull, L.D. McFadden, tectonic geomorphology north and south of the Garlock fault, California, in: D.O. Doehring (Ed.), Geomorphology in Arid Regions, A Proc. Vol. 8th Annu. Geomorphol. Symp., 1977, pp. 115–138, accessed April 13, 2022, https://www.scirp.org/(S(i43dyn45teexjx455qlt3d2q))/reference/ReferencesPapers.aspx?ReferenceID=1794102.
[12] P.G. Silva, J.L. Goy, C. Zazo, T. Bardají, Faulth-generated mountain fronts in southeast Spain: geomorphologic assessment of tectonic and seismic activity, Geomorphology 50 (2003) 203–225.
[13] J.V. Pérez-peña, A. Azor, J. Miguel, E.A. Keller, Geomorphology active tectonics in the Sierra Nevada (Betic Cordillera, SE Spain): insights from geomorphic indexes and drainage pattern analysis, Geomorphology 119 (2010) 74–87.
[14] F. Troiani, J.P. Galve, D. Piacentini, M. Della Seta, J. Guerrero, Spatial analysis of stream length-gradient (SL) index for detecting hillslope processes: a case of the Gállego River headwaters (Central Pyrenees, Spain), Geomorphology 214 (2014) 183–197.
[15] A. Pedrera, J.V. Pérez-Peña, J. Galindo-Zaldívar, J.M. Azañón, A. Azor, Testing the sensitivity of geomorphic indices in areas of low-rate active folding (eastern Betic Cordillera, Spain), Geomorphology 105 (2009) 218–231.
[16] M.T. Ramírez-Herrera, Geomorphic assessment of active tectonics in the acambay graben, Mexican volcanic belt, Earth Surf. Process. Landforms 23 (1998) 317–332.
[17] J.V. Pérez-Peña, J.M. Azañón, A. Azor, CalHypso: an ArcGIS extension to calculate hypsometric curves and their statistical moments. Applications to drainage basin analysis in SE Spain, Comput. Geosci. 35 (2009) 1214–1223.
[18] L. Andreani, K.P. Stanek, R. Gloaguen, O. Krentz, L. Domínguez-González, DEM-based analysis of interactions between tectonics and landscapes in the ore mountains and eger rift (East Germany and NW Czech Republic), Rem. Sens. 6 (2014) 7971–8001.
[19] J.V. Pérez-Peña, M. Al-Awabdeh, J.M. Azañón, J.P. Galve, G. Booth-Rea, D. Notti, SwathProfiler and NProfiler: two new ArcGIS add-ins for the automatic extraction of swath and normalized river profiles, Comput. Geosci. 104 (2017) 135–150.
[20] Z.T. Al-Attar, A.A. Othman, S.H.S. Al-Hakari, A.K. Obaid, S.G. Salar, V. Liesenberg, A neotectonic statistical assessment through watershed geomorphic analysis: a case study in the Greater Zab River Basin, Turkey–Iraq, Environ. Earth Sci. 81 (2022) 355–381, https://doi.org/10.1007/s12665-022-10478-7.
[21] V. Zygouri, I.K. Koukouvelas, S. Kokkalas, P. Xypolias, G.A. Papadopoulos, Geomorphology the Nisi Fault as a key structure for understanding the active deformation of the NW Peloponnese, Greece, Geomorphology (2013) 142–156.

[22] I.K. Koukouvelas, V. Zygouri, K. Nikolakopoulos, S. Verroios, Treatise on the tectonic geomorphology of active faults: the significance of using a universal digital elevation model, J. Struct. Geol. (2018) 241–252.
[23] H. Daxberger, R. Dalumpines, D.M. Scott, U. Riller, The ValleyMorph Tool: an automated extraction tool for transverse topographic symmetry (T-) factor and valley width to valley height (Vf-) ratio, Comput. Geosci. 70 (2014) 154–163.
[24] V.N. Scotti, P. Molin, C. Faccenna, M. Soligo, A. Casas-Sainz, The influence of surface and tectonic processes on landscape evolution of the Iberian Chain (Spain): quantitative geomorphological analysis and geochronology, Geomorphology 206 (2014) 37–57.
[25] A. Moussi, N. Rebaï, A. Chaieb, A. Saâdi, GIS-based analysis of the Stream Length-Gradient Index for evaluating effects of active tectonics: a case study of Enfidha (North-East of Tunisia), Arabian J. Geosci. 11 (2018) 123–138.
[26] S. Siddiqui, D. Castaldini, M. Soldati, DEM-based drainage network analysis using steepness and Hack SL indices to identify areas of differential uplift in Emilia–Romagna Apennines, northern Italy, Arabian J. Geosci. 10 (2017) 1–23.
[27] F. Shahzad, R. Gloaguen, TecDEM: a MATLAB based toolbox for tectonic geomorphology, Part 1: drainage network preprocessing and stream profile analysis, Comput. Geosci. 37 (2011) 250–260.
[28] N.K. Jaiswara, S.K. Kotluri, P. Pandey, A.K. Pandey, MATLAB functions for extracting hypsometry, stream-length gradient index, steepness index, chi gradient of channel and swath profiles from digital elevation model (DEM) and other spatial data for landscape characterisation, Appl. Comput. Geosci. 7 (2020), 100033.
[29] D. Piacentini, F. Troiani, T. Servizi, O. Nesci, F. Veneri, SLiX: a GIS toolbox to support along-stream knickzones detection through the computation and mapping of the stream length-gradient (SL) Index, 2020, pp. 1–14.
[30] G.L. Queiroz, E. Salamuni, E.R. Nascimento, Computers & geosciences knickpoint finder : a software tool that improves neotectonic analysis, Comput. Geosci. 76 (2015) 80–87.
[31] K.H. Karim, Z.A. Taha, Origin of limestone conglomerate in Dokan area, Iraqi Bull. Geol. Min. 8 (2012) 1–11.
[32] A. Dohan, S. Al-Hazaa, Sedimentological study of Dokan conglomerate in Kalakan anicline /NE Iraq, Kirkuk Univ. Journal-Scientific Stud. 14 (2019) 192–204.
[33] S.H.S. Al-Hakari, Paleostress analysis from brittle failure and minor structures in Dokan area, Kurdistan region, NE of Iraq, J. Zankoy Sulaimani - Part A. 18 (2016) 283–310.
[34] M. sh. Al-Kubaisi, A.H. Ward, Geometry of Khalakan Anticline, northeastern Iraq, Tikrit J. Pure Sci. 23 (2018) 1662–1813.
[35] A.K.S. Bety, Discrimination different lithological units using a remote sensing application: a case study in the Dokan area, Kurdistan Region – Iraq, J Water Land Devel 55 (2022) 109–114.
[36] I.S. Al-Jumaily, S.I. Al-khatoni, Fault-slip analysis and Paleostress reconstruction at sara anticline- Dokan dam site northeastern Iraq, Iraqi Natl. J. Earth Sci. 13 (2013) 75–102.
[37] M.S. Al-Kubaisi, J.M. Barno, Fold geometry and kinematics of inversion tectonics for Kosrat anticline, northeastern Iraq, Arabian J. Geosci. 8 (2015) 9469–9480.
[38] V.K. Sissakian, H.A. Al-musawi, N. Al-ansari, K. Sven, The origin and genesis of the Dokan conglomerate, NE Iraq, J. Earth Sci. Geotech. Eng. 6 (2016) 1–15.
[39] V.K. Sissakian, A.D.A. Ahad, N. Al-Ansari, R. Hassan, S. Knutsson, The regional Geology of Dokan area, NE Iraq, J. Earth Sci. Geotech. Eng. 6 (2016) 1792–9660.
[40] M. Al-Kubaisi, A. Ward, Structural development of Khalakan anticline and deposition of Dokan conglomerate, northeastern Iraq, Tikrit J. Pure Sci. 23 (2018) 87–96.
[41] S.H. Ahmed, Designation and study of anticlines-Kurdistan region-NE Iraq, J. Phys. Conf. Ser. 1294 (2019).
[42] S. Al-khatony, N. Al-Azzawi, F. Lawa, Structural and tectonic study of qara sard anticline and Choplagh syncline, from sulaimaniya area, Kurdistan region, northeastern Iraq, Iraqi Natl. J. Earth Sci. 19 (2019) 39–58.
[43] S.H. Ahmed, É. Barrier, C. Müller, Basin evolution model during cretaceous in the northeastern of Arabian plate in Kurdistan region Basin evolution model during cretaceous in the northeastern of Arabian plate in Kurdistan region, Arabian J. Geosci. (2016) 1–23.
[44] M. Alavi, Regional stratigraphy of the Zagros fold-thrust belt of Iran and its proforeland evolution, Am. J. Sci. 304 (2004) 1–20.
[45] V.K. Sissakian, Geological evolution of the Iraqi Mesopotamia Foredeep, inner platform and near surroundings of the Arabian Plate, J. Asian Earth Sci. 72 (2013) 152–163.
[46] S.F. Fouad, Tectonic map of Iraq, scale 1 : 1000,000, 3rd edition, 2012, Iraqi Bull. Geol. Min. 11 (2015) 1–7.
[47] Saad Z. Jassim, Jeremy C. Goff, Geology of Iraq, Dolin, Hlavni 2732, Prague and Moravinan Museum, Zelny trh6, Brno, Czech Republic, 2006.
[48] H. Seybold, W.R. Berghuijs, J.P. Prancevic, J.W. Kirchner, Global dominance of tectonics over climate in shaping river longitudinal profiles, Nat. Geosci. 14 (2021) 503–507.
[49] A.C. Whittaker, S.J. Boulton, Tectonic and climatic controls on knickpoint retreat rates and landscape response times, J. Geophys. Res. Earth Surf. 117 (2012) 1–19.
[50] M. Berberian, Master "blind" thrust faults hidden under the Zagros folds: active basement tectonics and surface morphotectonics, Tectonophysics 241 (1995) 193–224.
[51] M. Alavi, Tectonostratigraphic synthesis and structural style of the Alborz mountain system in Northern Iran, J. Geodyn. 21 (1996) 1–33.
[52] M. Allen, J. Jackson, R. Walker, Late Cenozoic Reorganization of the Arabia-Eurasia Collision and the Comparison of Short-Term and Long-Term Deformation Rates, 2004, pp. 1–16.
[53] F. Vernant, P. Nilforoushan, F. Hatzfeld, D. Abbassi, M.R. Vigny, C. Masson, F. Tavakoli, Present-day crustal deformation and plate kinematics in the Middle East constrained by GPS measurements in Iran and northern Oman, Geophys, J. Intell. 157 (2004) 381–398.
[54] G.F. Sella, T.H. Dixon, A. Mao, REVEL: A model for recent plate velocities from space geodesy, J. Geophys. Res. Solid Earth 107 (2002) 1–30. ETG 11-1-ETG 11-30.
[55] W. Abdulnaby, Structural Geology and Neotectonics of Iraq, Northwest Zagros, 2019, pp. 53–73.
[56] R.I. Koshnaw, B.K. Horton, D.F. Stockli, D.E. Barber, M.Y. Tamar-Agha, J.J. Kendall, Neogene shortening and exhumation of the Zagros fold-thrust belt and foreland basin in the Kurdistan region of northern Iraq, Tectonophysics 694 (2017) 332–355.
[57] M. Zebari, F. Preusser, C. Grützner, P. Navabpour, K. Ustaszewski, Late Pleistocene-Holocene slip rates in the northwestern Zagros mountains (Kurdistan region of Iraq) Derived from luminescence dating of river terraces and structural modeling, Tectonics 40 (2021) 1–24.
[58] V.K. Sissakian, N. Al-Ansari, L.H. Abdullah, Neotectonic activity using geomorphological features in the Iraqi Kurdistan region, Geotech. Geol. Eng. 38 (2020) 4889–4904.
[59] N.M.S. Numan, A plate tectonic scenario for the phanerozoic succession in Iraq, Iraqi Geol. J. 30 (1997) 85–119.
[60] S.K. Varoujan, Geomorphology and morphometry of the Greaterzab river basin ,north of Iraq, Iraqi Bull. Geol. Min. 9 (2013) 21–49.
[61] V.K. Sissakian, S.F.A. Fouad, Geological map of Iraq, scale 1 : 1000 000, 4th edition, 2012, Iraqi Bull. Geol. Min. 11 (2015) 9–17.
[62] M. Oehlers, K. McClay, J. De Vera, J. Gines, Structure of the Zagro fold and thrust belt in the Kurdistan region, northern Iraq, Trab. Geol. 29 (2009) 213–217.
[63] M.S. Ameen, Possible forced folding in the Taurus–Zagros belt of northern Iraq, Geol. Mag. 128 (1991) 561–584.
[64] M.M. Zebari, C.M. Burberry, 4-D evolution of anticlines and implications for hydrocarbon exploration within the Zagros fold-thrust belt, Kurdistan region, Iraq, GeoArabia. 20 (2015) 161–188.
[65] J.A. Jackson, Reactivation of basement faults and crustal shortening in orogenic belts, Nature 283 (1980) 343–346.
[66] J.A. Jackson, T.J. Fitch, D.P. McKenzie, Active thrusting and the evolution of the Zagros fold belt, Geol. Soc. Spec. Publ. 9 (1981) 371–379.
[67] Jamal A.H. Doski, Basement fault reactivation in the Zakho–Silopi region, Iraqi kurdistan – Turkey border, J. Univ. Duhok 20 (2017) 13–30.
[68] S. Kokkalas, E. Kamberis, P. Xypolias, S. Sotiropoulos, I. Koukouvelas, Coexistence of thin-and thick-skinned tectonics in zakynthos area (Western Greece): insights from seismic sections and regional seismicity, Tectonophysics 597–598 (2013) 73–84.
[69] S. Alsinawi, H.A.A. Ghalib, Historical seismicity of Iraq, Bull. Seismol. Soc. Am. 65 (1975) 541–547.

[70] Khalid J. Fahmi, Mazin A.H. Al Salim, Basil S. Ayar, Recent earthquake activity in the lesser zab region of northeastern Iraq, Tectonophysics 131 (1986) 89–111.
[71] T. Onur, R. Gök, W. Abdulnaby, H. Mahdi, N.M.S. Numan, H. Al-Shukri, A.M. Shakir, H.K. Chlaib, T.H. Ameen, N.A. Abd, A comprehensive earthquake catalog for Iraq in terms of moment magnitude, Seismol Res. Lett. 88 (2017) 798–811.
[72] W. Abdulnaby, K. Motaghi, E. Shabanian, H. Mahdi, H. Al-Shukri, R. Gök, Crustal structure of the mesopotamian plain, east of Iraq, Tectonics 39 (2020), 0–3.
[73] N.A.J. And, H.J.M. Nawal, A. Al-Ridah, Seismotectonic study of middle and southern Iraq, Iraqi Geol. J. 50 (2017).
[74] M. Font, D. Amorese, J.L. Lagarde, DEM and GIS analysis of the stream gradient index to evaluate effects of tectonics: the Normandy intraplate area (NW France), Geomorphology 119 (2010) 172–180.
[75] R.T.O.M. Cox, Analysis of Drainage-Basin Symmetry as a Rapid Technique to Identify Areas of Possible Quaternary Tilt-Block Tectonics : an example from the Mississippi Embayment, Geol. Soc. Am. Bull. (1994) 571–581.
[76] F.P.-A.F.M., U. P. Bailey, J. McKean, New techniques and metrics for describing rivers using high resolution digital elevation models AGU Fall Meet. Abstr. (2013) EP43C-0869.
[77] N.M. Gasparini, G.C. Fischer, J.M. Adams, N.H. Dawers, A.M. Janoff, Morphological signatures of normal faulting in low-gradient Alluvial rivers in South-Eastern, Earth Surf. Process. Landforms 41 (2016) 642–657.
[78] J. Petrovszki, G. Timár, Geomorphology Channel sinuosity of the Körös River system, Hungary/Romania , as possible indicator of the neotectonic activity, Geomorphology 122 (2010) 223–230.
[79] A. Zámolyi, B. Székely, E. Draganits, G. Timár, Geomorphology Neotectonic control on river sinuosity at the western margin of the little Hungarian plain, Geomorphology 122 (2010) 231–243.
[80] R.A. van Zuidam, F.I. van Zuidam-Cancelado, Terrain analysis and classification using aerial photographs : a geomorphological approach, in: ITC Textb. Photo-Interpretation, 1979, p. 310.
[81] R. El Hamdouni, C. Irigaray, T. Fernández, J. Chacón, E.A. Keller, Assessment of relative active tectonics, southwest border of the Sierra Nevada (southern Spain), Geomorphology 96 (2008) 150–173.
[82] V.K. Sissakian, L.H. Abdullah, Lateral growth of Safeen anticline as deduced from drainage analysis, Iraqi Kurdistan region, Kuwait J. Sci. (2023). Under publ.
[83] L.A. Ramsey, R.T. Walker, J. Jackson, Fold evolution and drainage development in the Zagros mountains of Fars province, SE Iran, Basin Res. 20 (2008) 23–48.
[84] A. Demoulin, Testing the Tectonic Significance of Some Parameters of Longitudinal River Profiles : the Case of the Ardenne ž Belgium , NW Europe/, 1998.
[85] J. Holbrook, S.A. Schumm, Geomorphic and sedimentary response of rivers to tectonic deformation: a brief review and critique of a tool for recognizing subtle epeirogenic deformation in modern and ancient settings, Tectonophysics 305 (1999) 287–306.
[86] S.K. Lahiri, R. Sinha, Geomorphology Tectonic controls on the morphodynamics of the Brahmaputra River system in the upper Assam valley, India, Geomorphology 169–170 (2012) 74–85.
[87] W. Viveen, R. Braucher, D. Bourlès, J.M. Schoorl, A. Veldkamp, R.T. Van Balen, J. Wallinga, D. Fernandez-mosquera, J.R. Vidal-romani, J. Sanjurjo-sanchez, A 0.65 Ma chronology and incision rate assessment of the NW Iberian Miño river terraces based on 10 Be and luminescence dating, Global Planet. Change 94–95 (2012) 82–100.
[88] L. Goren, M. Fox, S.D. Willett, Earth surface tectonics from fluvial topography using formal linear inversion: theory and applications to the Inyo mountains California, J. Geophys. Res. (2014) 1651–1681.
[89] J.T. Hack, Stream-Profile analysis and stream-gradient index, J. Res. U.S. Geol. Surv. 1 (1973) 421–429.
[90] J.M. Salvany, Tilting neotectonics of the Guadiamar drainage basin, SW Spain, Earth Surf. Process. Landforms 29 (2004) 145–160.
[91] S. Sboras, A. Ganas, S. Pavlides, S. Sboras, A. Ganas, S. Pavlides, Bulletin of the geological society of Greece morphotectonic analysis of the neotectonic and active faults of Beotia (Central Greece) 43 (2010) 1607–1618.
[92] M.S. Alshayef, A. Javed, Assessment of relative tectonics activity zones in Masila oil field, Yemen, J. Geovisualization Spat. Anal. 4 (2020) 1–17.
[93] A. Sanakhan, A. Solgi, A. Sorbi, M. Arian, Survey of active tectonic: the influence of river morphotectonic in Aras Basin, Arabian J. Geosci. 13 (2020).
[94] D.W. Burbank, J.K. Mclean, M. Bullen, K.Y. Abdrakhmatov, M.M. Miller, Partitioning of Intermontane Basins by Thrust-Related Folding, Tien Shan, Kyrgyzstan, 1999, pp. 75–92.
[95] M. Dehbozorgi, M. Pourkermani, M. Arian, A.A. Matkan, H. Motamedi, A. Hosseiniasl, Quantitative analysis of relative tectonic activity in the Sarvestan area, central Zagros, Iran, Geomorphology 121 (2010) 329–341.
[96] J. Holbrook, S.A. Schunun, Geomorphic and sedimentary response of rivers to tectonic deformation : a brief review and critique of a tool for recognizing subtle epeirogenic deformation in modern and ancient settings 305 (1999) 287–306.
[97] S. Ouchi, Response of Alluvial Rivers to Slow Active Tectonic Movement, 1985.
[98] J. Adams, Active tilting of the United States midcontinent: geodetic and geomorphic evidence, Geology 8 (1980) 442–446.
[99] S.A. Schumm, River response to baselevel change : implications for sequence stratigraphy 101 (1993) 279–294.
[100] J. Petrovszki, B. Székely, G. Timár, A systematic overview of the coincidences of river sinuosity changes and tectonically active structures in the Pannonian Basin, Global Planet. Change 98–99 (2012) 109–121.
[101] M.S. Al-kubaisi, M.A. Hussein, Morphotectonics of shatt Al-Arab river southern Iraq, Iraqi J. Sci. 55 (2014) 1051–1060.
[102] H.S. and Campbell J.K. Al-Daghastani, The evolution of the lower Waipara river gorge in response to active folding in north Canterbury, New Zealand, ITC J. 3 (1995) 246–255.
[103] K. McClay, J. De Vera, J. Gines, M. Oehlers, Structure of the Zagros fold and thrust belt in the Kurdistan region , northern Iraq, Trab. Geol. 29 (2009) 213–217.
[104] S.A. Schumm, OF ALLUVIAL RIVERS, Ann. Rev. Earth Planet. Sci. 13 (1985) 5–27.
[105] V.K. Sissakian, S.F. Fouad. Geological Map of Erbil and Mahabad Quadrangles, scale 1: 250000. Baghdad, 2nd edition, 2014.